



OPEN

SUBJECT AREAS:

GEOPHYSICS

CONDENSED-MATTER PHYSICS

Received

18 August 2014

Accepted

19 January 2015

Published

13 February 2015

Correspondence and requests for materials should be addressed to N.F. (funamori@eps.s.u-tokyo.ac.jp)

* Current Address: Deutsches Elektronen Synchrotron, Photon Science, 22607 Hamburg, Germany, and Precursory Research for Embryonic Science and Technology, Japan Science and Technology Agency, Tokyo 102-0075, Japan.

† Current Address: Department of Physics, Kyoto University, Kyoto 606-8502, Japan.

Muonium in Stishovite: Implications for the Possible Existence of Neutral Atomic Hydrogen in the Earth's Deep Mantle

Nobumasa Funamori¹, Kenji M. Kojima², Daisuke Wakabayashi¹, Tomoko Sato³, Takashi Taniguchi⁴, Norimasa Nishiyama^{5*}, Tetsuo Irifune^{5,6}, Dai Tomono^{7†}, Teiichiro Matsuzaki⁷, Masanori Miyazaki², Masatoshi Hiraishi², Akihiro Koda² & Ryosuke Kadono²

¹Department of Earth and Planetary Science, University of Tokyo, Tokyo 113-0033, Japan, ²Muon Science Laboratory, Institute of Materials Structure Science, High Energy Accelerator Research Organization, Tsukuba 305-0801, Japan, ³Department of Earth and Planetary Systems Science, Hiroshima University, Higashi-Hiroshima 739-8526, Japan, ⁴National Institute for Materials Science, Tsukuba 305-0044, Japan, ⁵Geodynamics Research Center, Ehime University, Matsuyama 790-8577, Japan, ⁶Earth-Life Science Institute, Tokyo Institute of Technology, Tokyo 152-8550, Japan, ⁷Nishina Center for Accelerator-Based Science, RIKEN, Wako 351-0198, Japan.

Hydrogen in the Earth's deep interior has been thought to exist as a hydroxyl group in high-pressure minerals. We present Muon Spin Rotation experiments on SiO₂ stishovite, which is an archetypal high-pressure mineral. Positive muon (which can be considered as a light isotope of proton) implanted in stishovite was found to capture electron to form muonium (corresponding to neutral hydrogen). The hyperfine-coupling parameter and the relaxation rate of spin polarization of muonium in stishovite were measured to be very large, suggesting that muonium is squeezed in small and anisotropic interstitial voids without binding to silicon or oxygen. These results imply that hydrogen may also exist in the form of neutral atomic hydrogen in the deep mantle.

Hydrogen is the most abundant element in the solar system. It binds to oxygen and the resultant water makes the Earth a habitable blue planet. Ocean covers 70% of the Earth's surface. Moreover, a significant amount of water may be hidden in the Earth's interior. The water in anhydrous silicates is considered to be related to lattice defects and incorporated into the system, for example, by simultaneous substitutions such as Mg²⁺ → H⁺ and O²⁻ → OH⁻ (Ref. 1). If a structural change is induced by significant substitutions, the system should be classified in hydrous silicates. In the field of earth science, the water in anhydrous silicates has been studied mainly by the methods to probe the oscillation of hydroxyl group, such as infrared absorption and Raman scattering²⁻⁵. It has been reported that the mantle-transition zone can accommodate a significant amount of H₂O component up to several times as much as the total mass of ocean¹ and, although it is not a consensus⁴, the lower mantle could also accommodate a non-negligible amount³.

At the same time, one can speculate that hydrogen might exist in silicates without substitutions. In the field of applied physics, hydrogen in perfect crystals of low-pressure phases of SiO₂ has been studied by the methods to probe H more directly⁶⁻¹⁰, such as Muon Spin Rotation (μSR) and Electron Paramagnetic Resonance (EPR), to obtain a better understanding of Metal-Oxide-Semiconductor (MOS) devices. In those studies, it has been reported that hydrogen can exist in interstitial voids of structure. Moreover, it has recently been revealed that a significant amount of small molecules, such as H₂ and He, dissolves into interstitial voids of low-pressure phases of SiO₂ (Refs. 11–15). Therefore, it seems possible that the hydrogen which is not directly related to lattice defects of silicates and has not so far been recognized sufficiently in earth science may exist in the mantle. However, because interstitial voids of low-pressure phases of SiO₂ are large, the above findings could be exceptional. The structures of two important SiO₂ minerals, stishovite and quartz, are compared in Figure 1. Stishovite is a rutile-type high-pressure phase and quartz is an ambient-pressure phase. The two structures show marked contrast in interstitial voids, in addition to the well-known difference in coordination number.

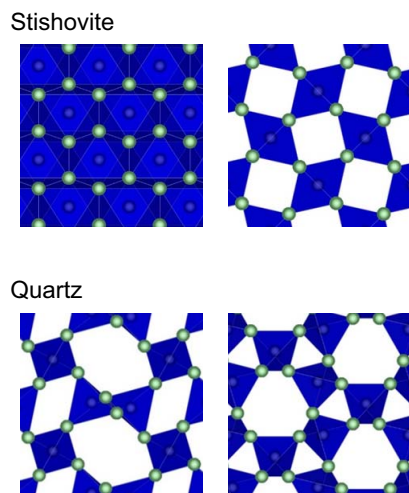


Figure 1 | Crystal structures of stishovite and quartz. They are archetypal high-pressure six-fold coordinated and low-pressure four-fold coordinated minerals having the same chemical formula of SiO_2 . View from the direction of crystallographic a-axis (left) and c-axis (right) is shown for the both structures.

Here, we present the results of μSR spectroscopy to show the possible existence of neutral atomic hydrogen in small and anisotropic interstitial voids of stishovite. Although μSR spectroscopy is not very popular in earth science, it is a well-established technique to simulate the behavior of hydrogen in semiconductors and insulators^{16,17}. Positive muon can be considered as a light isotope of proton with a mass of about 1/9 that of proton. In μSR , spin-polarized positive muons are implanted into matter and their subsequent behaviors (changes in spin polarization with time) are measured under various conditions of magnetic field. μSR is a powerful tool to probe the position, electronic state, and other information of the hydrogen that exists irregularly in matter, because it tracks the behavior of each implanted particle (in contrast to diffraction). In this study, μSR was conducted on powder and pellet samples to clarify intrinsic properties of stishovite (see Methods).

Results

An example of the time evolution of muon-spin polarization in stishovite powder is shown in Figure 2a. These spectra were measured at a transverse field of 350 G (nominal) at TRIUMF (Canada). The upper and lower limits of the vertical axis of the graph correspond to the amplitude for fully spin-polarized muons. This figure clearly indicates that the fraction of muon staying in the initial diamagnetic state (corresponding to OH forming hydrogen) is small. The muon fraction in stishovite increased slightly with decreasing temperature; 14% at 300 K, 14% at 250 K, 15% at 200 K, 16% at 150 K, 17% at 100 K, 17% at 50 K, and 19% at 2.5 K in stishovite powder.

The spectrum at 300 K in Figure 2a is enlarged in terms of the horizontal axis and is compared with quartz in Figure 2b,c. High-frequency oscillation of muonium-spin polarization is seen. The fraction of muonium (= muon-electron bound paramagnetic state, corresponding to neutral atomic hydrogen) can be determined from the amplitude of oscillation at time = 0 after subtracting the contribution of muon-spin polarization. Only the triplet state, in which muon and electron have spins of the same direction, appears in these spectra and the singlet state, in which they have spins of the opposite direction, has the same population as the triplet and does not appear; twice the amplitude of the triplet state corresponds to the fraction of muonium^{16,17}. It was determined to be 56% in stishovite at 300 K. The sum of muon and muonium fractions is smaller than 100%

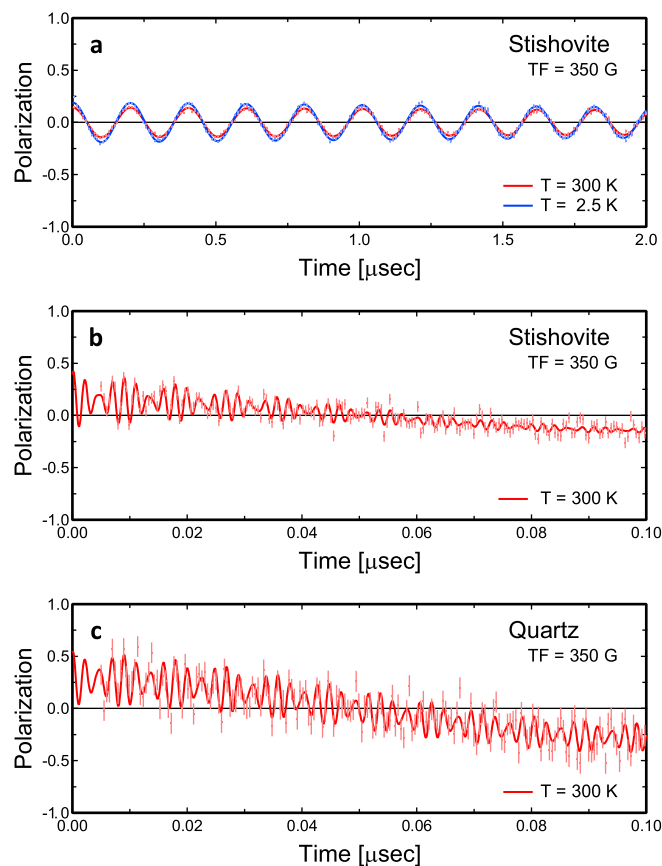


Figure 2 | Time evolution of muon- and muonium-spin polarization in stishovite and quartz. $P(t)$'s are plotted (Eq. 11). (a) Muon spin in stishovite powder taken at 300 K and 2.5 K under a transverse field of 350 G (nominal). (b and c) Muonium spin in stishovite and quartz powders. The spectrum at 300 K in (a) is enlarged in terms of the time axis and is shown again in (b) for stishovite. The vertical bars represent the statistical error (standard deviation) of each point.

(Table 1). The remaining 30% was missing due to fast relaxation in spin polarization. These spectra also show that the relaxation rate of muonium-spin polarization in stishovite is large.

The beat of oscillation due to the splitting of the triplet state under transverse field is also seen in Figure 2b,c. The frequencies determined from the spectrum for stishovite are 452(10) and 562(32) MHz. The hyperfine-coupling parameter of muonium A/h , where h is the Planck constant, can be determined from these frequencies. A/h 's for powder and pellet samples agree well with each other (Table 1). A/h for muonium in stishovite at 300 K is determined to be 4.67(3) GHz with all the spectra for the two samples at transverse fields from 200 to 1000 G (nominal). A/h at 2.5 K is 5.17(14) GHz, estimated only from the two frequencies at 350 G (nominal). These values are significantly larger than 4.49(2) GHz in quartz (Table 1) and 4.463 GHz in vacuum¹⁸. Data for stishovite plotted on the Breit-Rabi diagram^{16,17} are shown in Figure 3.

Experimental results at TRIUMF are summarized in Table 1. In both powder and pellet samples of stishovite, the muon fraction was small and decreased with increasing temperature. Also, A/h 's are the same for the two samples as mentioned above. On the other hand, some differences are found; the muon fraction and the relaxation rate of muonium-spin polarization were smaller in powder than in pellet. In this study, experiments were also conducted at RIKEN/RAL (UK), PSI (Switzerland), and MLF/J-PARC (Japan). Preliminary results at these facilities, such as the muon fraction and A/h in stishovite powder (roughly estimated based on decoupling measurements under

Table 1 | Summary of μ SR measurements for stishovite^a

Material	Form	Temperature [K]	Statistics [events]	f_{μ} [%]	λ_{μ} [μs^{-1}]	f_{Mu} [%]	λ_{Mu} [μs^{-1}]	A/h [GHz]
Stishovite	Powder	300	100 M	14.4(3)	0.10(1)	56(5)	24(4)	4.65(2)
		2.5	100 M	19.2(4)	0.13(1)	– ^b	– ^b	5.17(14)
	Pellet ^c	300	100 M	32.1(5)	0.05(1)	55(9)	55(9)	4.68(5)
		2.5	25 M	39.6(8)	0.06(1)	–	–	–
Quartz	Powder	300	25 M	28.0(6)	0.01(1)	56(8)	7(5)	4.49(2)

^a f_{μ} : fraction of muon, λ_{μ} : relaxation rate of muon, f_{Mu} : fraction of muonium, λ_{Mu} : relaxation rate of muonium, A/h: hyperfine-coupling parameter of muonium, where h is the Planck constant (see Methods for more details). Measurements shown in Figure 3 were used to determine A/h for stishovite and measurements at 350 and 700 G (nominal) were used to determine A/h for quartz. Measurements at 350 G (nominal) were used to determine the other parameters.

^bAlthough the simultaneous determination of f_{Mu} and λ_{Mu} was not successful due to the very fast relaxation, the relation between the two parameters can be expressed well as $f_{\text{Mu}} = 0.83\lambda_{\text{Mu}} + 8.1$.

^cSintered nanocrystals (Ref. 28).

longitudinal field), do not contradict those at TRIUMF described above. Experimental results for quartz are consistent with previous work^{6–8,10}.

A large muonium fraction was found in stishovite as is the case in quartz. Interstitial voids of stishovite, which consists of SiO_6 octahedra, are much smaller than those of quartz, which consists of SiO_4 tetrahedra (Fig. 1). Therefore, the present results suggest that the formation of muonium is not controlled by the size of interstitial voids. In stishovite, not only the muonium fraction was large but also the muon fraction decreased with increasing temperature, suggesting that implanted muons become more stable by capturing an electron to form muonium than by staying in diamagnetic state. Hyperfine-coupling parameter is a measure of 1s electronic orbital size; the cube of Bohr radius is inversely proportional to this parameter^{16,17}. Therefore, a very large hyperfine-coupling parameter of muonium in stishovite, which is even larger than that in quartz, suggests that muonium is squeezed in small interstitial voids without binding to silicon or oxygen. A very large relaxation rate of muonium-spin polarization cannot be explained by the effect of nuclear magnetic moments of silicon and oxygen because they are small. It may be due to anisotropy in hyperfine interactions. This explanation seems plausible because the relaxation rate becomes larger at low temperatures where the mobility of muoniums becomes smaller. In fact,

interstitial voids in stishovite are largely anisotropic (i.e., having channels along the c-axis; Fig. 1).

The difference in muonium fraction and relaxation rate of muonium-spin polarization between powder and pellet suggests that they are affected by the grain size and/or surface condition (= defects, in a broad sense) of samples. The pellet sample is a sintered body of nanocrystals and therefore has a much smaller grain size than the powder sample. A negative correlation between grain size and muon fraction may be explained by the inhibition of delayed-muonium formation, in which positive muons capture radiolysis electrons and become muoniums after time = 0 (Ref. 10). In quartz single crystal, it has been reported that muon and muonium fractions were 20% and 80%, respectively, and about the half of muonium was formed promptly after time = 0 (as delayed muoniums)¹⁰. On the other hand, in quartz powder, the muon fraction was 28% (Table 1). Therefore, a negative correlation between grain size and muon fraction is also seen in quartz. The delayed formation of muonium substantially (but very shortly) after time = 0 causes the de-phasing of spin polarization. This may explain the missing fraction in powder and pellet samples; i.e., the sum of muon and muonium fractions is smaller than 100% (Table 1). At low temperatures, the muon fraction becomes larger probably because the mobility of radiolysis electrons becomes smaller and therefore the formation of delayed muonium is inhibited. In any case, muonium seems to be more easily formed at higher temperatures and/or in more perfect crystals of stishovite.

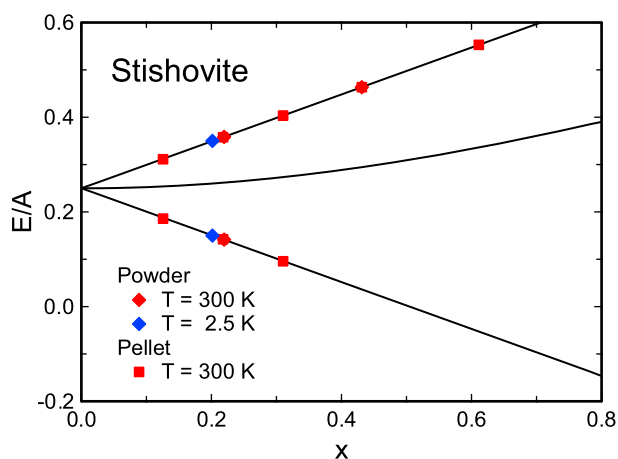


Figure 3 | Energy diagram of muonium in stishovite as a function of applied transverse field, so called Breit-Rabi diagram^{16,17}. x denotes the transverse field that is normalized by the field corresponding to A/h (Eq. 8). The three solid lines, in order from top to bottom, represent theoretical E_1/A , E_2/A , and E_3/A (Eqs. 12–14). The data of E_1/A and E_3/A , from left to right, correspond to the measurements at 200, 350, 500, 700, and 1000 G (nominal). Because of a larger A/h at 2.5 K than at 300 K, the data for 2.5 K are located at the left side of corresponding data at 300 K.

Discussion

In this study, μ SR experiments have suggested that the neutral atomic hydrogen (corresponding to muonium) can exist in stishovite without having a direct relation to lattice defects. So, the question is whether invisible hydrogen really exists in stishovite, i.e., without being detected by infrared absorption, Raman scattering, and other standard methods. Although proving the existence is difficult, a clue can be found in a report on MOS devices¹⁹. Infrared absorption due to Si-OH and Si-H oscillations was detected in γ -ray irradiated SiO_2 films of MOS devices, while it was not detected in non-irradiated films. It has been interpreted as a sign that H and/or H_2 released from an electrode of the device (hydrogen source) exist in the film and react with dangling bonds of silicon and oxygen generated by the γ -ray irradiation. Therefore, we believe that invisible hydrogen exists similarly in stishovite if hydrogen sources are available. However, even in the presence of hydrogen sources, oxidizing environment would favor the incorporation of water into stishovite by a substitution of $\text{Si}^{4+} \rightarrow 4\text{H}^+$ (Ref. 5). The situation may be similar in other high-pressure silicates. In previous studies of earth science, oxidizing environment has often been assumed and many experiments have been conducted in various silicate-water systems. However, the redox state of the deep mantle (from past to present) is a challenging issue^{20–23} and it may be much more reducing compared to the present shallow mantle^{20–22}.



Now we assume reducing environment in the deep mantle. Then, the question is whether hydrogen sources are available in the Earth's interior. A candidate may be the core. In some models of early earth evolution, a tremendous amount of hydrogen dissolved into the core^{2,24}. Or, hydrogen may have dissolved directly into the mantle at an early stage and stay there quietly^{20–22}; the chemoaffinity between silicates and liquid H₂ under high pressure has been demonstrated recently²⁵. Therefore, it is possible that the neutral atomic hydrogen which is not directly related to lattice defects of silicates may exist in the mantle. To further test the hypothesis, μ SR experiments should be conducted on more realistic mantle minerals and rocks. In-situ experiments under high pressure and high temperature are also indispensable. Definitely, studies from multiple viewpoints are required to know how much hydrogen can dissolve into silicates in a thermodynamically stable state. For example, accurate calculation of the formation enthalpy should be made with the help of knowledge obtained by experimental work. Neutral atomic hydrogen in the mantle will be an important research target in future earth science, because the existence form of this important element has a fundamental importance in physicochemical properties of mantle minerals, thus controls the dynamics and evolution of our planet.

Methods

Sample preparation. μ SR spectroscopy requires a relatively large amount of samples. So, nominally anhydrous stishovite samples were synthesized under high pressure and high temperature with a belt-type large-volume press²⁶ at National Institute for Materials Science (Japan) and with a Kawai-type large-volume press²⁷ at Geodynamics Research Center of Ehime University (Japan), respectively. To clarify intrinsic properties of stishovite, two kinds of samples were prepared; powder sample was synthesized with a standard technique at the former institute and pellet sample (sintered nanocrystals)²⁸ was synthesized with a recently developed technique at the latter institute. Stishovite powder of about 0.5 g was synthesized from noncrystalline SiO₂ powder (Kanto Chemical Co., Inc., purity 99.9%) at 10 GPa and 1373 K with the former press. For reference in μ SR experiments, quartz powder was also synthesized from the same starting material at 2 GPa and 1373 K with the same type of press. Each synthetic powder was packed in a capsule made of aluminum foil (having a thickness of 12 μ m). Stishovite pellet (sintered nanocrystals) of 5.5 mm in diameter and 1.0 mm in thickness was synthesized with the latter press. More detailed information on the stishovite pellet has been given elsewhere²⁸.

Experimental procedure. μ SR experiments were conducted for stishovite and quartz with surface-muon beams at RIKEN/RAL (UK), PSI (Switzerland), MLF/J-PARC (Japan), and TRIUMF (Canada). Spin-polarized positive muons were implanted into the capsulated powder or pellet and subsequent behaviors (changes in spin polarization with time) were measured under transverse magnetic field (perpendicular to the initial spin-polarization direction, up to 1000 G) or longitudinal magnetic field (parallel to the initial spin-polarization direction, up to 4000 G) at temperatures between 2.5 and 300 K (= room temperature). Stishovite powder was measured at all the four facilities and stishovite pellet was measured only at TRIUMF. Quartz powder was measured at MLF/J-PARC and TRIUMF. Based on preliminary results at RIKEN/RAL, PSI, and MLF/J-PARC, experiments with a high timing resolution, which is suitable for the observation of muonium, were conducted by using a continuous beam and a spectrometer called HiTime at TRIUMF.

Analytical procedure. Standard procedure was followed to analyze μ SR data^{16,17}. It is briefly summarized below.

First, data obtained with HiTime under transverse magnetic field were analyzed in frequency domain. Angular frequencies of muon-spin polarization ω_{\pm} and muonium-spin polarization ω_{Mu1} and ω_{Mu2} were determined by the Fourier transform. Because of the splitting of the triplet state, two frequencies appear for muonium. Thus determined ω_{\pm} and gyromagnetic ratio of muon γ_{μ} were used to determine the transverse magnetic field H actually applied to the sample with the equation

$$\omega_{\pm} = \gamma_{\mu} H. \quad (1)$$

Hyperfine-coupling parameter of muonium A/h relates to ω_{Mu1} and ω_{Mu2} with the following equations;

$$\frac{A}{h} = \frac{1}{2\pi} \frac{\omega_{+}^2 - (\omega_{-} - \omega_{Mu1})^2}{\omega_{-} - \omega_{Mu1}}, \quad (2)$$

$$\frac{A}{h} = \frac{1}{2\pi} \frac{\omega_{+}^2 - (\omega_{Mu2} - \omega_{-})^2}{\omega_{Mu2} - \omega_{-}}, \quad (3)$$

$$\omega_{\pm} = \frac{\gamma_e \pm \gamma_{\mu}}{2} H. \quad (4)$$

Here, h is the Planck constant and γ_e is the gyromagnetic ratio of electron. All the sets of (H, ω_{Mu1}) and (H, ω_{Mu2}) were used to determine A/h with a least-square method taking uncertainties in angular frequencies into account.

Next, data at 350 G (nominal) were analyzed in time domain with angular frequencies obtained by the Fourier transform. The equation

$$A(t) = A_{\mu} \cos(\omega_{\mu} t) \exp(-\lambda_{\mu} t) \quad (5)$$

was fitted to the data at time = 0.01 ~ 2.00 μ sec to determine amplitude A_{μ} and relaxation rate λ_{μ} of muon-spin polarization. Then, with fixed A_{μ} and λ_{μ} , the next equation was fitted to the data at time = 0.005 ~ 0.050 μ sec to determine amplitudes A_{Mu1} and A_{Mu2} and relaxation rate λ_{Mu} of muonium-spin polarization;

$$A(t) = A_{\mu} \cos(\omega_{\mu} t) \exp(-\lambda_{\mu} t) + [A_{Mu1} \cos(\omega_{Mu1} t + \phi) + A_{Mu2} \cos(\omega_{Mu2} t + \phi)] \exp(-\lambda_{Mu} t), \quad (6)$$

where

$$\frac{A_{Mu1}}{A_{Mu2}} = \frac{1+x+x^2}{1-x+x^2}, \quad (7)$$

$$x = \frac{\gamma_e + \gamma_{\mu}}{2\pi} H \frac{h}{A}. \quad (8)$$

Here, phase ϕ was introduced to correct the error in time = 0. The difference in relaxation rates of two frequencies was assumed to be negligible. Then, muon fraction f_{μ} and muonium fraction f_{Mu} were determined with the equations

$$f_{\mu} = \frac{A_{\mu}}{A_{Full}}, \quad (9)$$

$$f_{Mu} = \frac{2(A_{Mu1} + A_{Mu2})}{A_{Full}}. \quad (10)$$

Here, A_{Full} is the amplitude for fully spin-polarized muons, which was separately calibrated with Ag as a standard. ()' denotes that quantities in the parenthesis are corrected for the error in time = 0.

In Figures 2 and 3, time evolution of spin polarization P(t) and muonium ground-state energies E₁ and E₃ given below are presented.

$$P(t) = \frac{A(t)}{A_{Full}}, \quad (11)$$

and

$$E_1 = E_2 + \frac{1}{2\pi} h \omega_{Mu1}, \quad (12)$$

$$E_3 = E_2 - \frac{1}{2\pi} h \omega_{Mu2}, \quad (13)$$

where

$$E_2 = -\frac{1}{4} A + \sqrt{\frac{1}{4} A^2 + \left(\frac{1}{2\pi} h \omega_{+}\right)^2}. \quad (14)$$

- Smyth, J. R. β -Mg₂SiO₄: A potential host for water in the mantle? *Am. Mineral.* **72**, 1051–1055 (1987).
- Williams, Q. & Hemley, R. J. Hydrogen in the deep Earth. *Annu. Rev. Earth Planet. Sci.* **29**, 365–418 (2001).
- Murakami, M., Hirose, K., Yurimoto, H., Nakashima, S. & Takafuji, N. Water in Earth's lower mantle. *Science* **295**, 1885–1887 (2002).
- Bolfan-Casanova, N. Water in the Earth's mantle. *Mineral. Mag.* **69**, 229–257 (2005).
- Spektor, K. *et al.* Ultrahydrous stishovite from high-pressure hydrothermal treatment of SiO₂. *Proc. Natl. Acad. Sci. USA* **108**, 20918–20922 (2011).
- Myasishcheva, G. G., Obukhov, Yu. V., Roganov, V. S. & Firsov, V. G. A search for atomic muonium in chemically inert substances. *Sov. Phys. JETP* **26**, 298–301 (1968).
- Gurevich, I. I. *et al.* Muonium in magnetic field. *Phys. Lett.* **29B**, 387–390 (1969).
- Brown, J. A. *et al.* A precision determination of the hyperfine splitting of muonium in quartz. *Solid State Commun.* **33**, 613–614 (1980).
- Isoya, J., Weil, J. A. & Davis, P. H. EPR of atomic hydrogen ¹H and ²H in α -quartz. *J. Phys. Chem. Solids* **44**, 335–343 (1983).
- Brewer, J. H. *et al.* Delayed muonium formation in quartz. *Physica B* **289–290**, 425–427 (2000).



11. Sato, T., Funamori, N. & Yagi, T. Helium penetrates into silica glass and reduces its compressibility. *Nature Commun.* **2**, 345 (2011).
12. Shen, G. *et al.* Effect of helium on structure and compression behavior of SiO₂ glass. *Proc. Natl. Acad. Sci. USA* **108**, 6004–6007 (2011).
13. Efimchenko, V. S., Fedotov, V. K., Kuzovnikov, M. A., Zhuravlev, A. S. & Bulychev, B. M. Hydrogen solubility in amorphous silica at pressures up to 75 kbar. *J. Phys. Chem. B* **117**, 422–425 (2013).
14. Sato, T. *et al.* Anomalous behavior of cristobalite in helium under high pressure. *Phys. Chem. Miner.* **40**, 3–10 (2013).
15. Matsui, M., Sato, T. & Funamori, N. Crystal structures and stabilities of cristobalite-helium phases at high pressures. *Am. Mineral.* **99**, 184–189 (2014).
16. Schenck, A. *Muon Spin Rotation Spectroscopy: Principles and Applications in Solid State Physics* (Adam Hilger Ltd., Bristol and Boston 1985).
17. Yaouanc, A. & de Réotier, P. D. *Muon Spin Rotation, Relaxation, and Resonance: Applications to Condensed Matter* (Oxford University Press, Oxford 2011).
18. Liu, W. *et al.* High precision measurements of the ground state hyperfine structure interval of muonium and of the muon magnetic moment. *Phys. Rev. Lett.* **82**, 711–714 (1999).
19. Nagasawa, Y. *et al.* The study of the thermal oxide films on silicon wafers by Fourier transform infrared attenuated total reflection spectroscopy. *J. Appl. Phys.* **68**, 1429–1434 (1990).
20. Ballhaus, C. Is the upper mantle metal-saturated? *Earth Planet. Sci. Lett.* **132**, 75–86 (1995).
21. Rohrbach, A. *et al.* Metal saturation in the upper mantle. *Nature* **449**, 456–458 (2007).
22. Frost, D. J. & McCammon, C. A. The redox state of Earth's mantle. *Annu. Rev. Earth Planet. Sci.* **36**, 389–420 (2008).
23. Siebert, J., Badro, J., Antonangeli, D. & Ryerson, F. J. Terrestrial accretion under oxidizing conditions. *Science* **339**, 1194–1197 (2013).
24. Fukai, Y. The iron-water reaction and the evolution of the Earth. *Nature* **308**, 174–175 (1984).
25. Shinozaki, A. *et al.* Influence of H₂ fluid on the stability and dissolution of Mg₂SiO₄ forsterite under high pressure and high temperature. *Am. Mineral.* **98**, 1604–1609 (2013).
26. Kanke, Y., Akaishi, M., Yamaoka, S. & Taniguchi, T. Heater cell for materials synthesis and crystal growth in the large volume high pressure apparatus at 10 GPa. *Rev. Sci. Instrum.* **73**, 3268–3270 (2002).
27. Irifune, T., Isobe, F. & Shinmei, T. A novel large-volume Kawai-type apparatus and its application to the synthesis of sintered bodies of nano-polycrystalline diamond. *Phys. Earth Planet. Inter.* **228**, 255–261 (2014).
28. Nishiyama, N. *et al.* Synthesis of nanocrystalline bulk SiO₂ stishovite with very high toughness. *Scr. Mater.* **67**, 955–958 (2012).

Acknowledgments

μSR experiments were conducted at RIKEN/RAL, PSI, MLF/J-PARC, and TRIUMF. The authors are grateful to beam line staffs of these facilities for experimental support and K. Nishiyama, K. Shimomura, and S. Tsuneyuki for invaluable discussion on the muonium state in matter. This work was in part supported by a Grant-in-Aid for Scientific Research (Japan) and Special Coordination Funds for Promoting Science and Technology (Japan).

Author contributions

N.F., K.M.K., D.W., T.S., A.K. and R.K. designed the study. T.T., N.N. and T.I. prepared the samples. N.F., K.M.K., D.W., T.S., D.T., T.M., M.M., M.H., A.K. and R.K. conducted the μSR experiments and analyzed the data. N.F., K.M.K., D.W., T.S. and R.K. wrote the manuscript and others gave comments to improve the manuscript.

Additional information

Competing financial interests: The authors declare no competing financial interests.

How to cite this article: Funamori, N. *et al.* Muonium in Stishovite: Implications for the Possible Existence of Neutral Atomic Hydrogen in the Earth's Deep Mantle. *Sci. Rep.* **5**, 8437; DOI:10.1038/srep08437 (2015).



This work is licensed under a Creative Commons Attribution 4.0 International License. The images or other third party material in this article are included in the article's Creative Commons license, unless indicated otherwise in the credit line; if the material is not included under the Creative Commons license, users will need to obtain permission from the license holder in order to reproduce the material. To view a copy of this license, visit <http://creativecommons.org/licenses/by/4.0/>